

**FINAL TECHNICAL REPORT**

Grant Award Number: 05HQGR0012

**Recipient:**

Carlos Mendoza  
P.O. Box 693  
Golden, CO 80402  
Email: cmendoza33@msn.com

**Principal Investigators:**

Carlos Mendoza and William R. McCann

**Improving the Seismic Hazard Model for Puerto Rico through Seismic Tomography and a Reliable Microearthquake Catalog With Recalculated Magnitudes and Calibrated Hypocentral Error Estimates: Collaborative Research with W. McCann and C. Mendoza**

**Program Element:**

Element I: National and Regional Earthquake Hazard Assessments

*Research supported by the U.S. Geological Survey (USGS), Department of the Interior, under USGS award number 05HQGR0012. The views and conclusions contained in this document are those of the authors and should not be interpreted as necessarily representing the official policies, expressed or implied, of the U.S. Government.*

**Award Number 05HQGR0012**

***IMPROVING THE SEISMIC HAZARD MODEL FOR PUERTO RICO THROUGH SEISMIC TOMOGRAPHY AND A RELIABLE MICROEARTHQUAKE CATALOG WITH RECALCULATED MAGNITUDES AND CALIBRATED HYPOCENTRAL ERROR ESTIMATES: COLLABORATIVE RESEARCH WITH W. MCCANN AND C. MENDOZA***

**William R. McCann**  
10210 West 102<sup>nd</sup> Avenue  
Westminster, Colorado 80021  
Phone/Fax (303) 650-5484  
Email: wrmccann@comcast.net

**Carlos Mendoza**  
P.O. Box 693  
Golden, CO 80402  
Email: cmendoza33@msn.com

**Abstract**

Work conducted under the current project was aimed at improving the hazard model utility of the earthquake catalog of the Puerto Rico Seismic Network that monitors earthquake activity in the U.S. Caribbean (Puerto Rico and U.S. Virgin Islands). Data from that local seismic network were used to estimate the one-dimensional S-wave velocity structure and three-dimensional P-wave velocity structure for Puerto Rico. We identified a northerly dipping region of slower than normal seismic velocities extending from near the surface off the south coast to 50 kilometers depth. This feature lies just beneath a dipping zone of seismic activity of similar geometry. Together these results confirm the existence of the Muertos Megathrust, a major earthquake hazard for southern Puerto Rico. Other observations of the 3-D velocity model include identification of a region of high velocities in the region near the Utuado Batholith, and a region of low velocities near the north coast Tertiary basin.

We also developed a new duration magnitude scale calibrated to the moment estimates of Motazedian and Atkinson (2005) as well as a catalog of jointly located local earthquakes with new magnitudes.

## Introduction

Earthquake monitoring in the Puerto Rico-Virgin Islands (PRVI) region began in early 1975 with the installation of a northeastern Caribbean seismic network operated by Lamont-Doherty Earth Observatory (LDEO) and a western Puerto Rico network operated by the U.S. Geological Survey (USGS). The LDEO and USGS networks were combined after 1982 to form the Puerto Rico Seismic Network (PRSN) with operational responsibility transferred to the University of Puerto Rico. The net result of this operational history is that catalogs of events in the PRVI region contain earthquakes located with different location programs using different station configurations and different crustal-velocity models. The Puerto Rico Seismic Network (PRSN) is presently a local network of about 25 seismic stations. More than 18,000 earthquakes have been located by the PRSN to date, with most of these in the 1.0-3.0 magnitude range. The effort reported on herein develops a catalog of earthquakes located in a single 1-D velocity model with duration magnitudes recalculated using a moment-calibrated formulation. This catalog is the best to date for use in earthquake hazard models.

### 1-D *Velest* Vp/Vs model

More than 18,000 earthquakes have been located in the PRVI region since 1975, with most of them in the 1.0-3.0 magnitude range. In a recent study, McCann (2006) used the arrival-time data collected for these 18,000 events with the program *Velest* to jointly locate the earthquakes and develop an improved regional 1-D velocity model for the Puerto Rico region. This effort included a comparison of the real vs. model locations of numerous natural and artificial control events occurring from 1975-1979. *Velest* is a FORTRAN77 routine designed to derive 1-D velocity models for earthquake location procedures (Kissling, 1988, Kissling et al., 1994). The program started as Hypo2d (Ellsworth, 1977; Roecker, 1977) and has been recently modified to calculate a "Minimum 1-D Model" well suited for 1-D velocity model earthquake location programs. It has been successfully applied to local earthquakes and controlled source data in the western U.S. and Europe.

Table 1 shows the crustal velocity model obtained by McCann (2006) for the Puerto Rico region using *Velest*. This improved 1-D model and associated station delays (Table 2) form a "stable minimum residual dataset" that can be used to locate both past and future events registered by the local network. The new velocity model has been used to relocate all earthquakes in the Puerto Rico region recorded since 1975 to derive a unified earthquake catalog for use in the development of seismic-hazard models. The new, improved catalog allows a more complete assessment of the earthquake hazard and a better characterization of active faults.

**Table 1. 1-D *Velest* derived Vp, Vp/Vs velocity models for Puerto Rico and Virgin Islands**

Puerto Rico				Virgin Islands	
Vp (km/sec)	Vs (km/sec)	Vp/Vs	Depth to top of Layer (km)	Vp (km/sec)	Depth to Top of Layer (km)
6.45	3.59	1.80	-3	6.04	-3
7.13	4.15	1.72	17	6.43	9
8.01	4.59	1.74	31	7.50	24

**Table 2. Station Parameters Velest 1-D Model  
Puerto Rico Model AI, P and S-wave**

Sta	Phase	Nobs	Avres	Avwres	Std	Wsum	Delay (sec)
agp	P	11	-0.062	0.000	0.17	18	0.11
agp	S	10	-0.001	-0.003	0.13	3	0.17
apr	P	293	-0.005	0.000	0.23	470	0.05
apr	S	281	-0.008	0.002	0.20	80	0.00
cca	P	4	-0.008	0.000	0.16	6	-0.15
cca	S	4	0.002	-0.003	0.19	3	-0.22
cdp	P	7	-0.020	0.000	0.14	14	-0.23
cdp	S	7	-0.146	-0.001	0.27	10	-0.60
cpd	P	282	0.003	-0.001	0.22	449	-0.15
cpd	S	274	-0.040	-0.001	0.19	80	-0.25
csb	P	284	0.003	0.000	0.21	456	-0.26
csb	S	259	-0.010	-0.001	0.19	68	-0.33
cup	P	2	-0.104	-0.032	0.64	1	-1.51
ide	P	47	0.007	0.000	0.25	65	0.06
ide	S	22	-0.064	-0.001	0.19	6	0.05
imo	P	14	-0.041	0.013	0.30	17	0.15
imo	S	9	0.020	0.002	0.25	2	0.37
lpr	P	120	-0.007	-0.001	0.18	188	-0.27
lpr	S	119	0.006	-0.001	0.20	35	-0.47
lrs	P	310	-0.002	0.000	0.25	540	-0.26
lrs	S	289	0.034	0.000	0.20	86	-0.43
lsp	P	285	-0.006	0.001	0.23	480	0.00
lsp	S	235	-0.006	-0.001	0.22	62	0.11
mcp	P	48	0.009	0.009	0.16	74	-0.09
mcp	S	37	0.016	-0.001	0.18	9	-0.17
mep	P	22	-0.026	0.000	0.14	26	-0.13
mep	S	16	0.002	-0.004	0.15	3	-0.19
mgp	P	320	0.010	0.000	0.24	530	-0.01
mgp	S	285	-0.010	0.002	0.20	74	0.06
mov	P	4	0.007	0.000	0.12	6	-0.28
mov	S	4	0.008	-0.003	0.16	3	-0.22
mtp	P	2	-0.877	-0.024	0.22	2	-0.62
pnp	P	176	-0.015	-0.001	0.62	310	-0.04
pnp	S	163	-0.013	-0.004	0.37	46	-0.01
sjg	P	290	0.008	0.000	0.22	456	-0.21
sjg	S	283	-0.011	0.002	0.21	87	-0.24
sjv	P	2	-0.239	-0.016	0.04	2	-0.62
sjv	S	2	0.519	-0.004	0.11	1	-1.11
cbyp	P	73	0.009	0.000	0.28	131	-0.16
cbyp	S	67	-0.055	-0.001	0.21	17	-0.16
celp	P	174	-0.030	-0.022	0.25	305	-0.15
celp	S	175	-0.083	-0.093	0.16	49	-0.17

Sta	Phase	Nobs	Avres	Avwres	Std	Wsum	Delay (sec)
cllp	P	158	0.032	0.021	0.23	294	-0.15
cllp	S	154	0.113	0.096	0.15	46	-0.17
moca	P	64	0.009	0.002	0.46	107	0.52
moca	S	55	-0.015	0.002	0.32	13	0.79
porp	P	337	-0.002	0.000	0.25	587	-0.19
porp	S	321	-0.001	-0.001	0.17	87	-0.21
sjgc	P	7	-0.038	-0.045	0.11	8	-0.21
sjgc	S	7	-0.063	-0.046	0.22	5	-0.24

### Uncertainties in *Velest* 1-D Model

The *Velest* 1-D model and associated station delays obtained by McCann (2006) form a “stable minimum residual dataset” that can be used to locate both past and future events registered by local networks operated in Puerto Rico. We attempt to evaluate the validity of this improved seismic velocity model by examining the mislocation errors observed for artificial sources recorded in Puerto Rico since 1975. More than 60 quarry blasts were recorded in northeastern Puerto Rico between 1976 and 1978 that were included in the dataset used by McCann (2006) to derive the *Velest* 1-D model. The *Velest*-derived locations for these blasts are shown in Figure 1. These blasts were associated with quarrying operations at three different sites, but no information is available to unequivocally identify the site that corresponds to each blast. Figure 1, however, indicates that the absolute errors are not greater than 5 km and are generally less than 3 km for the majority of the blasts.

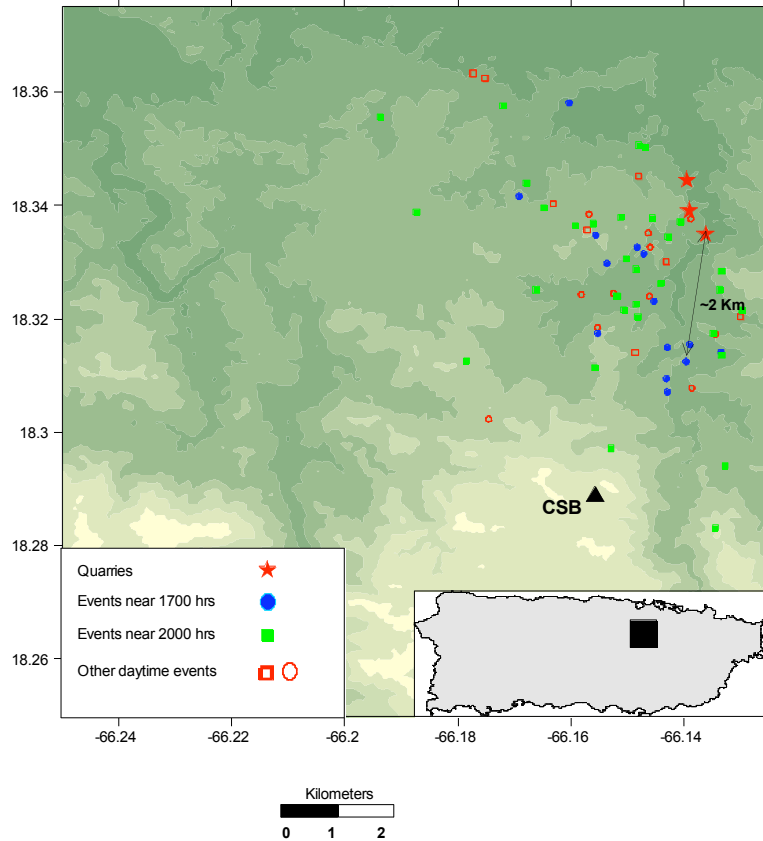


Figure 1. Epicentral locations obtained with *Velost* for 1976 to 1978 blasts in Puerto Rico relative to the three quarry locations (stars). P arrivals at station CSB were recorded for all of the blasts.

Mislocation errors shown in Figure 1 are presumably due to unknown variations in the velocity model, errors in the phase-arrival measurements, and the geographic distribution of the recording sites. We have used the computer program LOK developed by Zivcic and Ravnik (2002) to examine the possible contribution of each of these factors to the epicentral error. The program follows the method described by Peters and Crosson (1972) to construct hypocenter error ellipsoids for a uniform distribution of grid points encompassing a particular distribution of recording stations. Errors in the phase-arrival times and uncertainties in the velocity model are explicitly specified to derive location errors for each point along the regional grid. Mendoza and Huerfano (2005) used this program to estimate epicentral errors for earthquakes recorded by the current Puerto Rico network as a function of uncertainties in the velocity model.

LOK provides a measure of the epicentral error for a given station configuration assuming that all stations record the events. Thus, in order to compare with the absolute location errors shown in Figure 1, it was necessary to consider only those events that were located using either only P arrivals or both P and S arrivals from the same stations. Quarry blasts having more than 5 phase arrivals that fulfill either of these criteria are listed in Table 3. For events having both P and S readings, we assumed that the S arrivals correspond to pS phases that originate at or near the surface and have a travel time approximating that of the direct S wave.

**Table 3. Best-recorded Puerto Rico blasts, Naranjito Quadrangle**

Date	P-wave Arrivals	S-wave Arrivals	Velest Location	Mislocation Range, km
760206	6	0	18.342; -66.169	3.0 - 3.3
761112	8	0	18.324; -66.152	1.9 - 2.3
770426	7	0	18.331; -66.150	1.4 - 1.7
771019	5	5	18.338; -66.151	1.3 - 1.4
771208	5	5	18.314; -66.133	2.0 - 3.0

We examined the epicentral errors associated with the blasts from Table 3 by first assuming no uncertainty in the velocity model and no phase-reading errors to evaluate the effect of station configuration on the event location. The results of these initial tests indicate no contribution to the blast mislocation for these specific station distributions. Also, for all station distances, the P and S waves traverse only the upper layer of the 1-D velocity model, so that the *Velest* locations are affected only by velocity uncertainties within this top layer. In order to examine the effect of variations in velocity of the upper layer, we ran the program LOK assuming no errors in the measurement of the P and S arrivals. The results indicate that  $V_P$  and  $V_S$  uncertainties in the upper layer are limited to  $\pm 0.01$  km/sec. For all 5 blasts, P and S velocity uncertainties greater than this value yield epicentral errors much greater than the absolute location errors listed in Table 3. That is, the LOK results indicate that a velocity perturbation smaller than  $\pm 0.01$  km/sec in the upper layer is sufficient to account for the error in location observed for the blasts.

Mislocation errors may also be affected by errors in the timing of the phase arrivals, and we additionally run the program LOK for different prescribed values of phase-measurement errors assuming no velocity-model uncertainty. For events with both P and S arrivals, we assume that the S reading error is twice that of the P wave. The results indicate a linear increase in epicentral mislocation with increasing reading error. For example, for stations that recorded blasts 771019 and 771208, the P and S measurement errors (Figure 2) would have to be on the order of 0.035 sec and 0.07 sec, respectively, in order not to dramatically exceed the observed epicentral errors. Similar results were obtained for blasts having only P arrivals. For example, for the station distribution that recorded blast 761112, a P measurement error of 0.04 sec yields the observed maximum epicentral error of 2.3 km.

Since there is a direct tradeoff between phase-measurement errors and the uncertainty in the seismic velocities of the upper layer, these estimated phase-reading errors generally correspond to upper-bound estimates. Similarly, the inferred P and S velocity uncertainty of  $\pm 0.01$  km/sec would correspond to an upper-bound estimate for the top layer in the *Velest* 1-D model. These results based on the artificial sources indicate that the *Velest* velocities of the top layer are very well constrained. We are unable to conduct a similar velocity-uncertainty analysis for the lower layers because recording sites for the blasts were not sufficiently far away to sample the deeper depths.

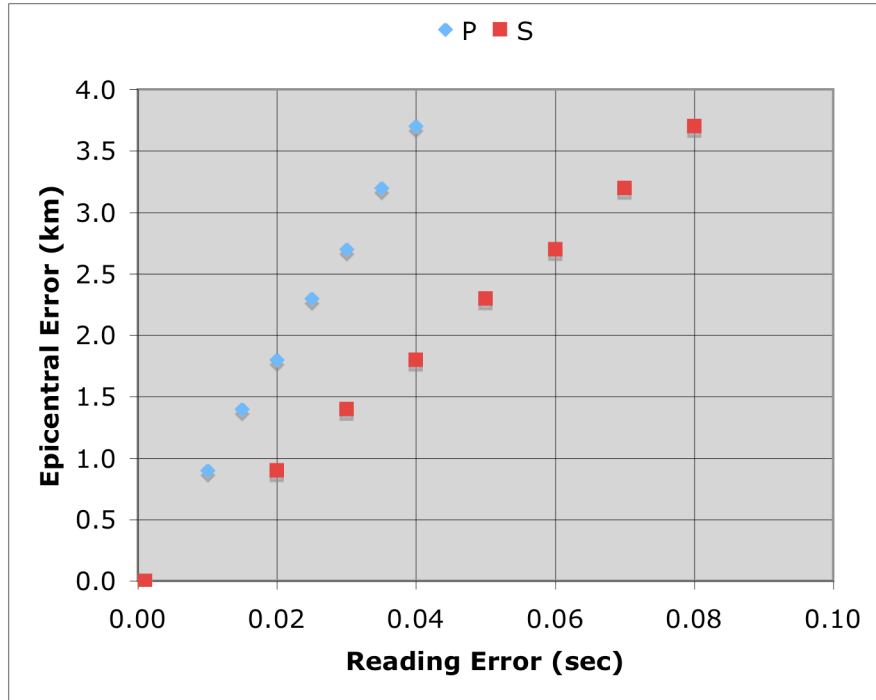


Figure 2. Expected epicentral errors calculated with LOK as a function of prescribed P and S reading error for the station configuration that recorded the 771019 and 771208 blasts. Calculations assume no uncertainty in the 1-D velocity model.

### 3-D Velocity Model

The *Velest* velocity model from Table 1 was additionally used to initiate the tomographic inversion process for the Puerto Rico region using the program *Simul2000* (Thurber, 1993). Figure 3 shows the area of study and the earthquake data used to derive the 3-D velocity structure. The depth interval considered for the study region is 100 km.

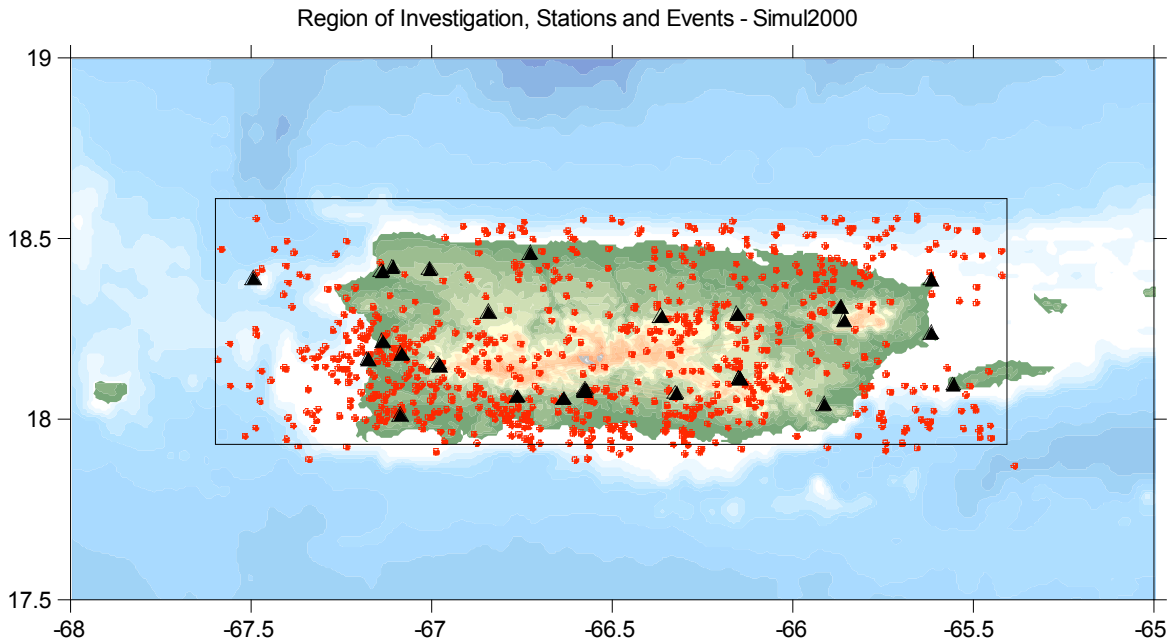


Figure 3. Location of 742 locally recorded earthquakes (at least 5 P-wave arrivals) with 4871 arrival times at 31 stations (black triangles) used to derive a 3-D velocity model using the program *Simul2000*. Box indicates region of investigation as determined by limits of nodes in velocity model.

The tomographic analysis was conducted in several steps. First, a mesh of coarse 3-D elements was defined across the length, width, and depth of the study region, and the inversion was run using the *Veleast* 1-D model as the starting model. This served to adjust the earthquake locations and 1-D velocity model to a 3-D structure. The inversion was then repeated iteratively using recomputed hypocenters until the best fit was obtained. In subsequent steps, the number of 3-D elements was incremented by progressively decreasing the size of each volume. In our analysis of the Puerto Rico earthquake data, the size of the 3-D elements was decreased from coarse (20-30 km node spacing) to medium (12 km node spacing) to fine (6 km node spacing).

Excessive computing times and lack of sufficient rays prohibited us from inverting for the fine node spacing throughout the region of Puerto Rico, so velocities at nodes in the deeper regions and the region to the east were held fixed at the coarse or medium node spacing during the last step of the inversion. In Figure 4 velocity anomalies at a series of horizontal layers are presented in the 4 upper panels. Depths for the layers are -1, 5, 11, and 17 km. Cooler colors represent P-wave velocities faster than the reference model, and warmer colors, slower velocities.

The most prominent features are the region of low velocities near the north central coast of the island and regions of higher than normal velocities just to the southwest and east. As there is a geographical overlap between these anomalies and at least portions of large geologic features, we tentatively correlate the region of low velocity with the north coast Tertiary basin (Larue et al., 1998), and the region of high velocity with the Utuado pluton (irregular polygon, figure 4; Jolley et al., 1998). In Figure 5 the Caribbean slab is seen as a North-South laterally extensive region of lower than normal velocities (as much as +3%) dipping to the north at mid- and lower crustal levels and shallow levels in the upper mantle. This low velocity feature represents the unusually thick crust of Caribbean Plate subducted beneath Puerto Rico.

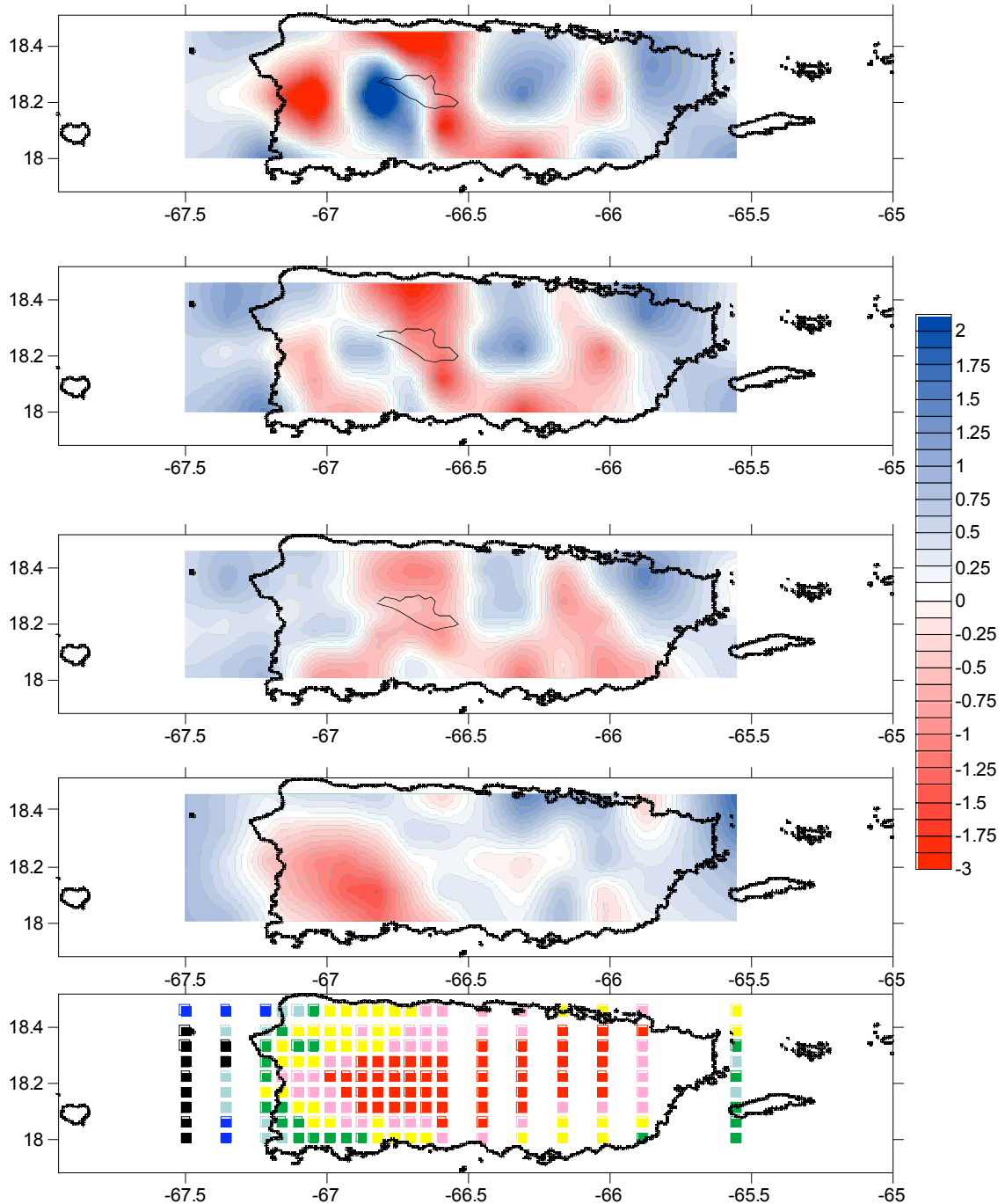
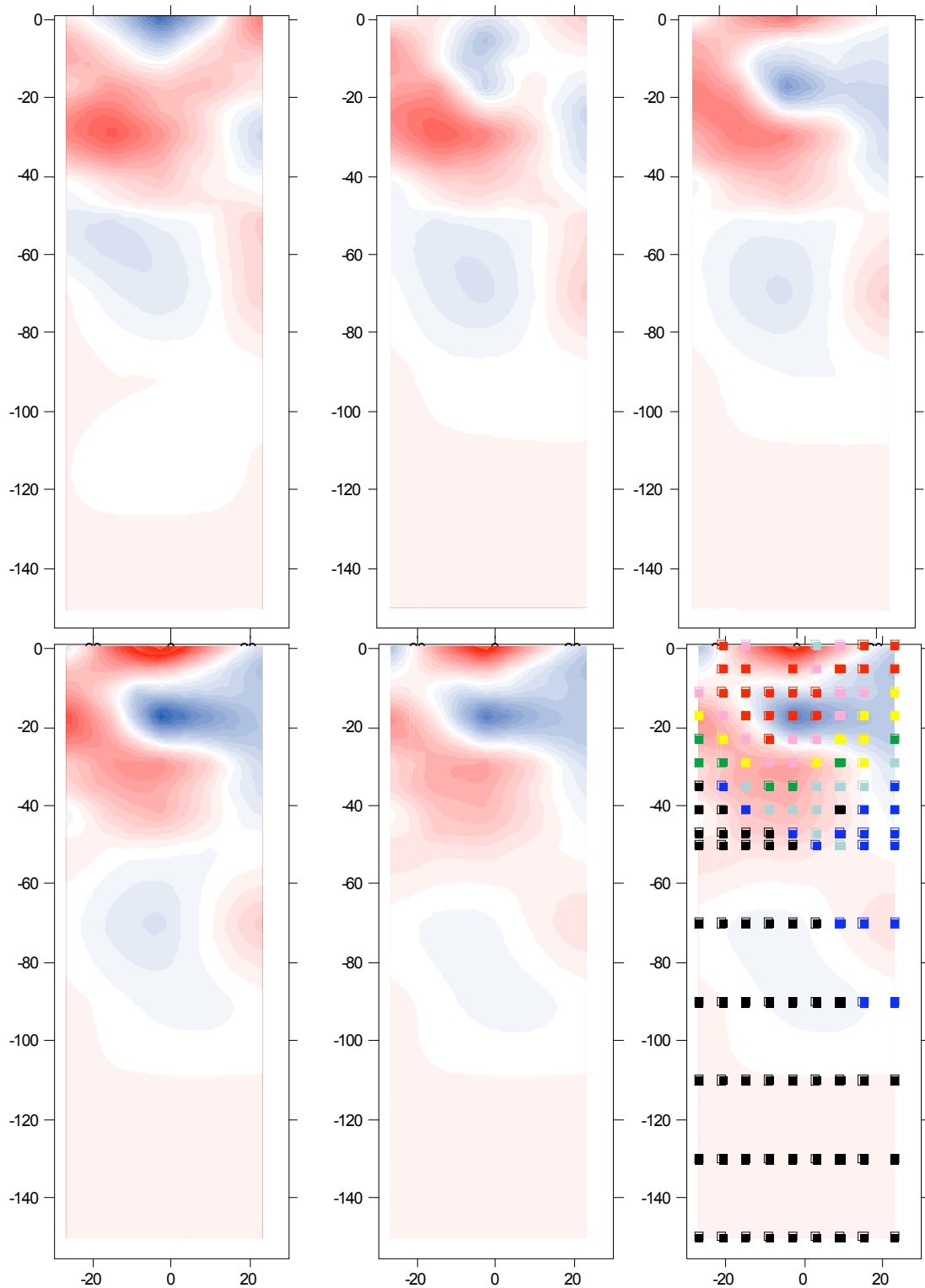


Figure 4. P-Velocity perturbation in the crustal portion of Puerto Rico. Upper four panels show P-wave velocity perturbation (in %) at depths of  $-1$ ,  $5$ ,  $11$ , and  $17$  km depth. The irregular polygon is the location of the Utuado Batholith. Note that perturbations in the central and eastern part of the island persist at least to  $17$  km depth, whereas the high velocity anomaly just to the west of the batholith does not even reach  $11$  km depth. At  $17$  km depth the most prominent feature is the wide region of slow velocities in the western part of the island. This is seen in the vertical cross section to be a northerly dipping structure identified as the crust of the subducted Caribbean plate. The lowermost panel shows the location of the nodes in the final iteration of the inversion. Note the higher density in the western part of the island. Colors indicate the number of hits at each node at layer  $-1$  km, Black is less than 5 hits. Blue is 5- 10 hits, and each successively warmer color represents a doubling in the number of hits. Red represents 160 – 320 hits.

The velocity perturbation extends to about 50 km depth where velocities gradually return to normal. At the upper surface of this region of lower than normal velocities lies a similarly dipping seismic zone, presumably reflecting the interface between the upper and lower plates. This observation is probably the most important result of this portion of the project i.e. verification of the existence of Caribbean plate, presumably subducted along the Muertos Trough, beneath southwestern Puerto Rico. The presence of this lithospheric slab and the interplate megathrust has clear implications for seismic hazard in the Puerto Rico region.



*Figure 5.* Several north-south sections through western Puerto Rico. Color schemes are as in figure 4. First 5 panels are sections at 66.87, 66.93, 66.99, 67.05, and 67.1 W. Last panels show the number of hits per node for the last section.

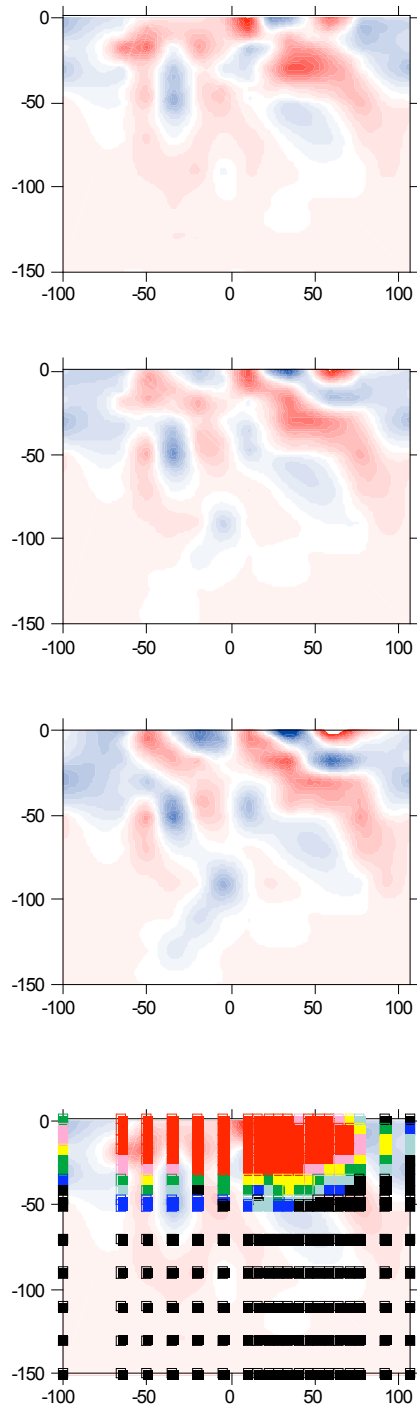
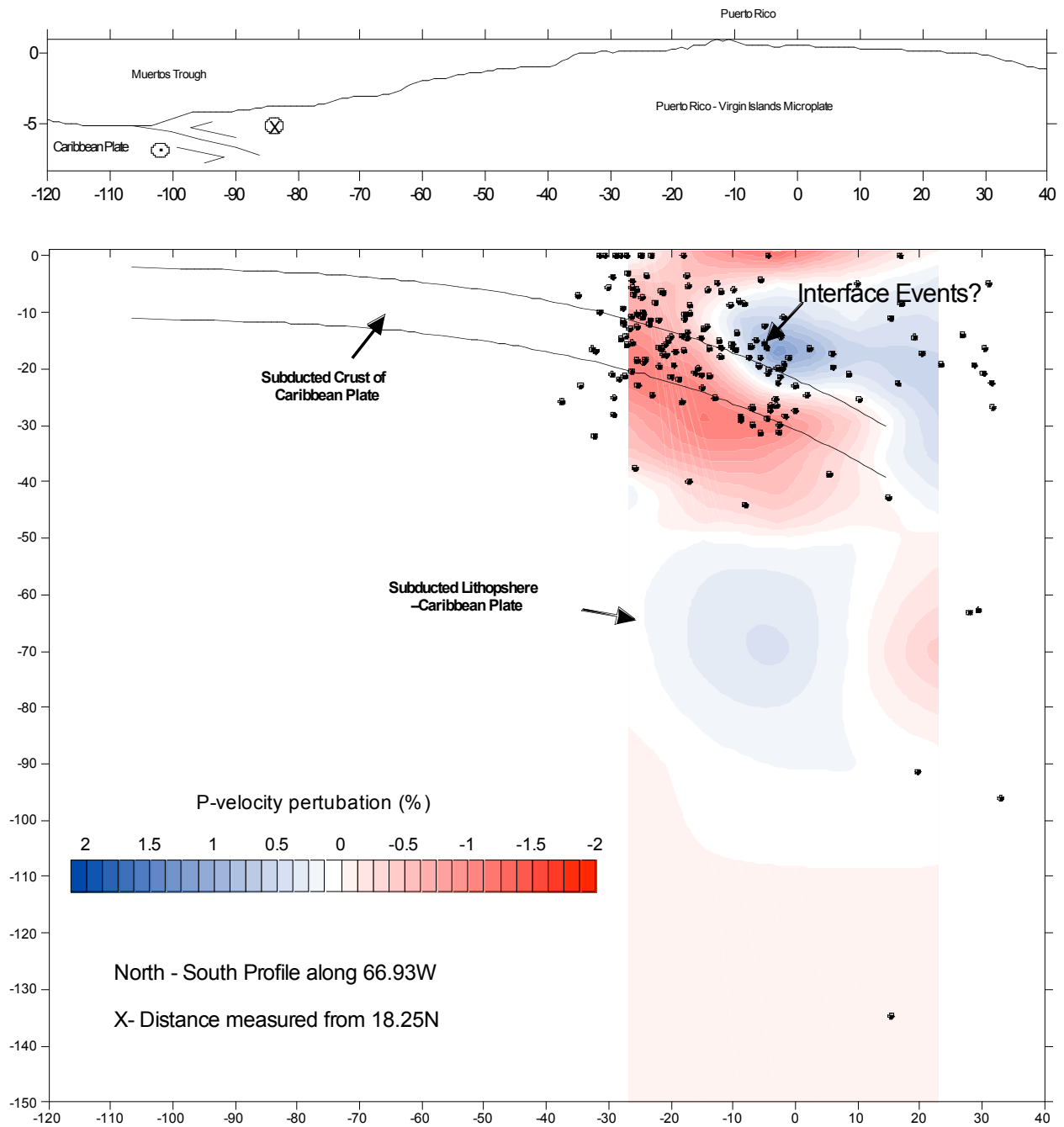


Figure 6. East-west sections as viewed from the north through southern Puerto Rico. Section are at 18.11, 18.16, and 18.22N. Lower panel shows number of hits for section at 18.11N. Color schemes are as in figure 4. Horizontal distances are measured from 66.5W



*Figure 7.* Upper panel: Regional relief (bathymetry and topography), location of plate boundaries (with motions derived from GPS) are shown for reference. Lower Panel: Percent  $V_p$  velocity variation from the standard model along a north-south striking vertical slice at 66.83°W. Also shown are *Velest* JHD earthquakes locations within 20 km of the profile center. The northerly dipping region of low velocity anomalies beneath S. Puerto Rico confirms the existence of subducted Caribbean slab beneath the island.

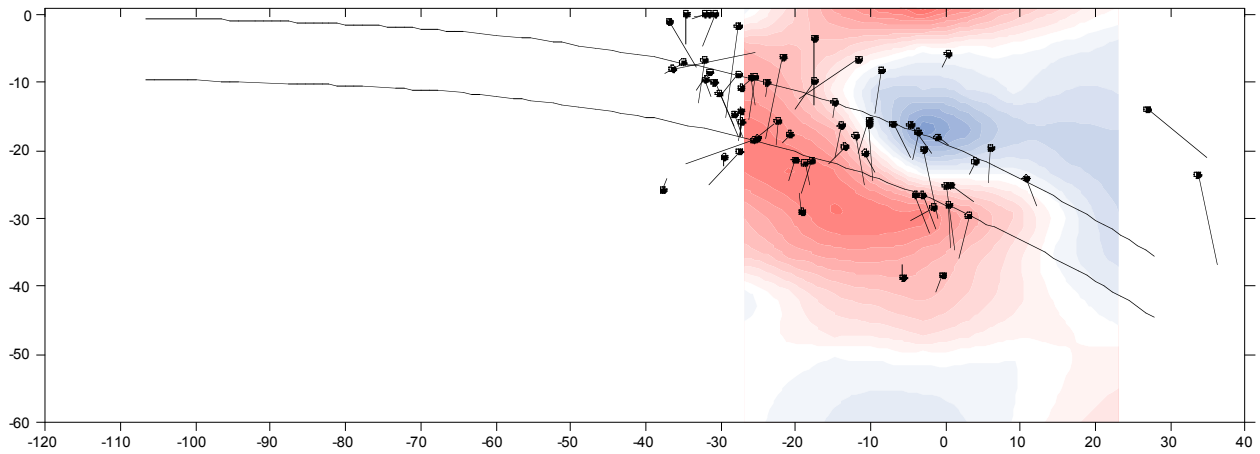


Figure 8. Details of the Muertos megathrust. Color scheme is as in figure 4 and represents P-wave velocity perturbations as discussed in text. Dots with lines are locations of selected events first located in the 1-D *Velest*  $V_p$  and  $V_s$  velocity models. Each event has 6 ts/tp,  $rms < 0.25$ , and is located between 66.0 and 67.5W; of those *Velest* events, some were used in the 3-D modeling and relocated. Those 78 events are shown here. The dot is 3-D location and the tail leads to the original *Velest* location. Events in general locate several kilometers shallower in the 3-D model. If the plate interface is adjusted upward (curved line) to coincide with the location of the interface events, the velocity anomaly coincides more with the upper mantle of the subducted plate rather than the thick subducted crust of the Caribbean Plate. In either case, the plate interface lies about 10 kilometers beneath southwestern Puerto Rico.

### A New Duration Magnitude Scale for Puerto Rico

The development of a new catalog of JHD earthquake locations using the phase data of the local network provides a new dataset of well-located locally recorded earthquakes for the period 1975- 2001. Recently, Motazedian and Atkinson (2005) used the local network waveforms to calculate  $M_1$ , a measure of moment magnitude for small to moderate earthquakes. They determined  $M_1$  for about 300 local and regional earthquakes, and while they did develop a relation between their moment magnitude,  $M_1$  and  $M_d$  the magnitude based on the coda duration measured by the local network,

$$M_1 = 0.76 M_d + 0.43 \quad (1)$$

use of this formulation would not allow recalculation of older network data whose magnitudes were determined using different magnitude - coda duration relations than is presently used by the network, nor could magnitude recalculation be done routinely in programs such as Hypoellipse and Hypoinverse, which use standard formulas to calculate magnitudes from coda observations.

Therefore, we developed a new coda duration magnitude scale calibrated to the Motazedian and Atkinson (2005)  $M_1$  observations following the standard *Hypoellipse* formulation for duration magnitudes,

$$M_d = C_1 + C_2 \log_{10}(F * c) + C_3 D + C_4 Z + C_5 (\log_{10}(F * c))^2 \quad (2)$$

where  $C_1$  through  $C_5$  are found empirically,  $F$  is the coda duration observed at a single station,  $c$  is the coda correction at that station,  $Z$  is event depth, and  $D$  is epicentral distance. (Lee and others, 1972; Lahr and other, 1975; Bakun and Lindh, 1977).

Motazedian and Atkinson (2005) calculated  $M_1$  for 302 local and regional earthquakes for the period 1993 through 2002. We searched the local network database for the period 1993 through May 31, 2001, (dataset available to us at the time) for coda observations of the events for which Motazedian and Atkinson (2005) calculated  $M_1$ . We found 1621 coda observations at 18 local network stations.

We determined  $C_1$  through  $C_5$  and  $c$  (for the 18 stations reporting) using a least squares procedure. As some of events used by Motazedian and Atkinson (2005) are far enough away from the network to make determination of their location using just local network data difficult, we used distances from the various stations to the epicenter as determined in the global catalog (NEIC).

Two cases were studied, one using the constants  $C_1$  through  $C_4$  (linear relation, equation 3) and another  $C_1$  through  $C_5$  (i.e. including the non linear term  $C_5$ , equation 4)

$$M_d = 0.14444 + 1.7638\text{Log}_{10}(F*c)+0.0008D+ -0.0003Z \quad (3)$$

$$M_d = 0.3816 + 1.4396\text{Log}_{10}(F*c)+0.0008D+ -0.0003Z+0.0206(\text{log}_{10}(F*c))^2 \quad (4)$$

Station corrections for the two cases are given in Table 4. Figures 9a and 9b show the new relations between observed moment magnitudes  $M_1$  and the new  $M_d$ .

**Table 4. Individual station corrections for the two *Hypoellipse* formulation cases studied. Correction is used to multiply observed coda duration.**

Code	Linear	Non-Linear	# Obs
agp	0.91	1.01	16
apr	0.98	1.08	144
cbyp	0.82	0.92	53
celp	0.85	0.92	147
cllp	0.84	0.88	25
cpd	0.89	1.01	157
csb	0.89	1.01	129
ide	1.42	1.55	20
imo	1.23	1.32	10
lpr	1.30	1.38	18
lrs	0.92	1.02	134
lsp	0.88	0.98	146
mcp	0.93	0.99	9
mgp	0.94	1.02	168
moca	1.00	1.07	62
pnp	0.92	1.04	38
porp	0.86	0.95	183
sjg	1.14	1.27	162

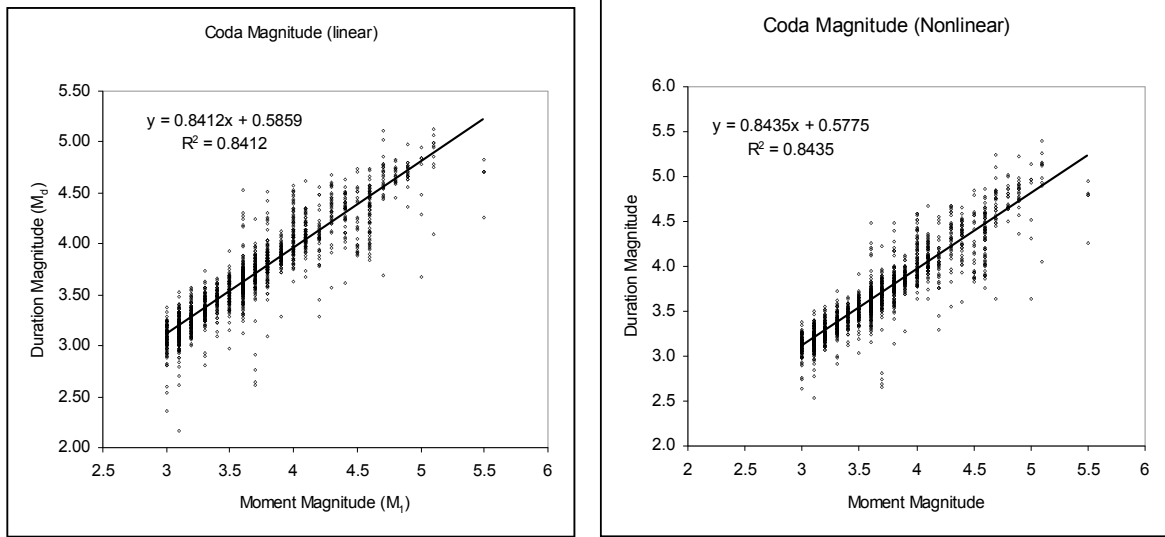


Figure 9a, 9b. Relations between moment magnitude ( $M_1$ ) and new duration magnitude ( $M_d$ ) using hypoellipse formulation. Note that the inclusion of the nonlinear term in the  $M_d$  formulation (figure 9b) leads to a better fit between  $M_1$  and  $M_d$  ( $R^2$  of .8412 vs. 8435).

We also developed an alternative scale consistent with the present network methodology for coda magnitude calculation using the formulation of Eaton (1992). Eaton (1992) uses a different formulation for duration-magnitude relation:

$$M_{fij} = 2.22(\log \tau_{ij} - \log \tau_0) + \log(\text{CAL}_{15}/\text{CAL}_i) + FC_i + FS_i + HF(h)_j \quad (5)$$

Where  $-2.22 \log \tau_0 = -0.81 + 0.0011 D_{ij} + 0.005 (D_{ij} - 40) D_{ij} < 40 \text{ km}$   
 $-2.22 \log \tau_0 = -0.81 + 0.0011 D_{ij} \quad 40 \text{ km} < D_{ij} < 350 \text{ km}$   
 $-2.22 \log \tau_0 = -0.81 + 0.0011 D_{ij} + 0.0006 (D_{ij} - 350) D_{ij} > 350.0 \text{ km}$   
 $HF(h)_j = 0.014 (h_j - 10.0) \text{ if } h_j > 10 \text{ km}$   
 $FC_i$  is MF component correction  
 $FS_i$  is MF site correction

We used that formulation to develop a separate set of equations for Puerto Rico calibrated by the Motazedian and Atkinson (2005)  $M_1$  observations along with the 1621 coda observation noted above. We assumed  $\log(\text{CAL}_{15}/\text{CAL}_i)$  to be zero as it represents a factor in station histories not available to us at this time.  $FC_i$  was also set to zero. We also found that variation of magnitude residuals varied little with distance or depth, generally less than 0.05 units with a standard deviation of 0.2. Therefore, the data do not appear to support complicated changes in formulas for certain ranges of distance or depth as was done by Eaton (1992). However, this issue should be investigated further. Site correction  $MF_i$  are given in Table 5. Given the caveats above, our constants derived through least squares fitting of the data lead to:

$$M_{fij} = 2.22 \log \tau_{ij} - .6359 + 0.0004 D_{ij} + FS_i - 0.0007 (h)_j \quad (6)$$

**Table 5. Individual Stations  $FS_i$ , corrections for Eaton formulation.  
Correction is added as in equation 6.**

Code	$FS_i$
agp	-0.13
apr	-0.05
cby	-0.18
cel	-0.16
clp	-0.36
cpd	-0.13
csb	-0.13
ide	0.24
imo	0.06
lpr	0.08
lrs	-0.10
lsp	-0.13
mcp	-0.23
mgp	-0.08
moca	0.01
pn	-0.08
por	-0.17
sj	0.07

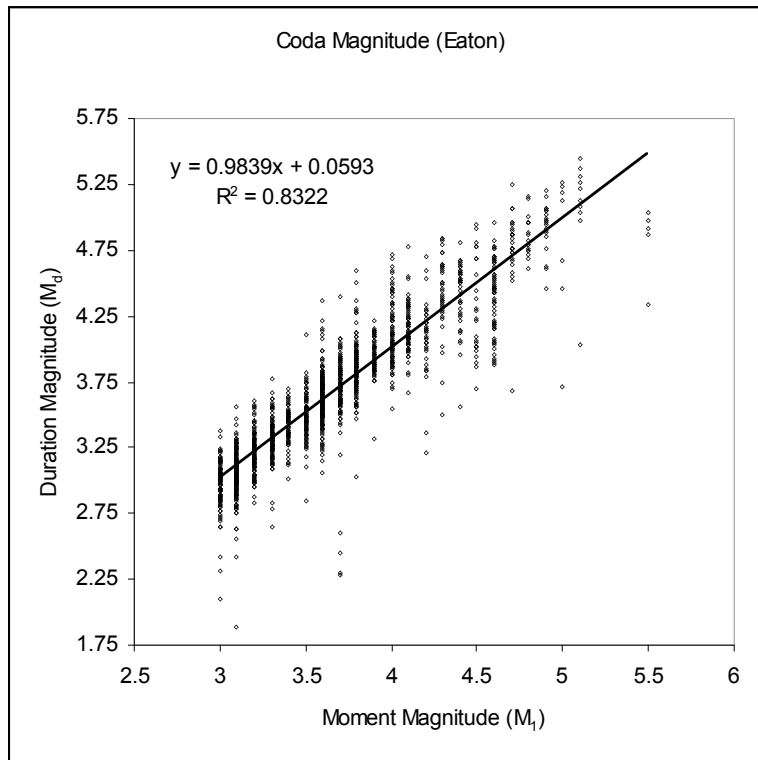


*Figure 10.* Relation between moment magnitude ( $M_1$ ) and new duration magnitude ( $M_d$ ) using Eaton formulation.

## **Summary**

Earthquake data recorded by the Puerto Rico Seismic Network have been used to estimate the three-dimensional P-wave velocity structure and the one-dimensional S-wave velocity structure in the Puerto Rico region. These data identify a zone of slower than normal seismic velocities that dips to the north from the south coast of Puerto Rico. This northerly-dipping, lower-velocity region lies just beneath a similarly-oriented zone of seismicity, confirming the existence of downgoing Caribbean lithosphere at the Muertos Trough. Additional structural features include a region of high velocities in the vicinity of the Utuado Batholith and a region of low velocities near the north coast Tertiary basin. The data have also been used to develop a new duration magnitude scale for Puerto Rico and a catalog of jointly located local earthquakes with recomputed magnitudes that can be used for earthquake hazard estimation in the Puerto Rico region.

## References

- Bakun, W. H. and A. G. Lindh, 1977, Local magnitudes, seismic moments and coda durations for earthquakes near Oroville, California, *Bull. Seism. Soc. Amer.*, 67, 615-629.
- Ellsworth, W., 1977, Three dimensional structure of the crust and mantle beneath the island of Hawaii, PhD Thesis, Mass. Inst. Tech.
- Jolly, W., E. Lidiak, J. Schellekens, and H. Santos, 1998, Volcanism, tectonics, and stratigraphic correlations in Puerto Rico, in eds., E. Lidiak and D. Larue, *Tectonics and Geochemistry of the NE Caribbean*, GSA Special Paper 322, 1-34.
- Kissling, E., 1988, Geotomography with local earthquake data, *Rev. Geophys.*, 26, 659-698.
- Kissling, E., Ellsworth, W., Ebert-Phillips, D., and U. Kradolfer, 1994, Initial reference models in local earthquake tomography, *J. Geophys. Res.*, 99, 19,635-19,646.
- Lahr, J. C., R. A. Page, and J. A. Thomas, 1975, Catalog of earthquakes in south central Alaska, April-June 1972, U.S. Geological Survey, Open-File Report, 30 p.
- Larue, D., R. Torrini, A. Smith and J. Joyce, North Coast Tertiary Basin of Puerto Rico: From Arc Basin to carbonate platform and arc-massif slope in eds., E. Lidiak and D. Larue, *Tectonics and Geochemistry of the NE Caribbean*, GSA Special Paper 322, 155-176.
- Lee, W. H. K., R. E. Bennett, and K. L. Meagher, 1972, A method of estimating magnitude of local earthquakes from signal duration: U.S. Geological Survey Open-File Report, 28 p.
- McCann, W., 2006, 1-D velocity models for Puerto Rico and the Virgin Islands, Northeastern Caribbean, to be submitted to *Bull. Seism. Soc. Amer.*
- Mendoza, C. and V. Huerfano, 2005, Earthquake location accuracy in the Puerto Rico-Virgin Islands region, *Seism. Res. Lett.*, 76, 356-363.
- Motazedian, D. and G. Atkinson, 2005, Earthquake magnitude measurements for Puerto Rico, *Bull. Seism. Soc. Amer.*, 95, 725-730.
- Peters D. C. and R. S. Crosson, 1972, Application of prediction analysis to hypocenter determination using a local larray, *Bull. Seism. Soc. Amer.*, 62, 775-788.
- Roecker S.W., 1977, Seismicity and tectonics of the Pamir-Hindu Kush region of central Asia, PhD Thesis, Mass. Inst. Tech.
- Thurber, C., 1993, Local earthquake tomography: velocities and  $V_p/V_s$  – theory, in *Seismic Tomography: Theory and Practice*, p. 563-583, Chapman and Hall, London.
- Zivcic M. and J. Ravnik, 2000, Detectability and earthquake location accuracy modeling of seismic networks, Appendix IS7.4 in ed., P. Bormann, *IASPEI New Manual of Seismological Observatory Practice* Potsdam, GeoForschungsZentrum, 1,252 p.